JOURNAL OF MATERIALS SCIENCE 28 (1993) 2315–2320

Radial distribution function analysis of coir fibre

D. N. MAHATO, B. K. MATHUR, S. BHATTACHERJEE
Department of Physics, Indian Institute of Technology, Kharagpur 721 302, India

Radial distribution analysis of X-ray intensities diffracted by natural coir fibre subjected to various thermal and mercerization treatments has been carried out. Interatomic distances, mean square displacements and interatomic coupling constants have been obtained from the radial distribution curves. As coir fibre finds its various applications in its natural form, its study has been carried out without disturbing the configuration of its cellulose–lignin complex during the treatments. Interatomic distances remain more or less the same during thermal and chemical treatments but the coupling constants and the mean square displacements experience changes, reflecting the changed mechanical behaviour of the fibre.

1. Introduction

Coir is a fruit fibre obtained from coconut palm (*Cocos nucifera*). It is found in tropical regions and plays a dominant role in the economy of the region. Some of the characteristics of the fibre have been studied by Varma *et al.* and the results have been reported in a series of publications [1–4]. Coir is mainly a multicellular fibre which contains 30 to 300 or more cells in its cross-section. Cells in natural fibres like coir refer to the crystalline cellulose arranged helically in a matrix consisting of a non-crystalline cellulose–lignin complex.

Coir has several valuable physical properties which stem from its structure. Among the most useful properties, mention may be made of length, fineness, strength, rigidity, wettability, resistivity [5], resistance to dampness etc. These properties make the coir fibre extremely useful for various domestic and commercial applications. Another important application, developed over the last few decades, is in preparing composites with different polymers [6]. In fact, intensive work has been going on for exploring possible utilization of coir and coir-composites in various new areas. In most of these applications coir fibre is used in its natural form. Hence a structural study of the natural fibre without disturbing the configuration of its cellulose–lignin complex will be more helpful, not only for better understanding of the structure but also for its applications to several purposes. The present paper reports the results of such a study on natural coir.

TABLE I Identification of observed d values of coir fibre with the corresponding lines of cellulose I [7, 8]

Line No.	Intensity	d (nm)		Cellulose-I indexing
		Observed	Calculated	
1	46	0.606	0.603	101
2	100	0.402	0.393	002
3	46	0.336	0.343	030
4	62	0.235	0.233	023
5	55	0.203	0.206	133
6	76	0.143	0.141	344
7	80	0.123	0.130	443
8	6	0.171		

2. Experimental procedure

Bristle native fibres were obtained by courtesy of the Central Coir Research Institute, Aleppe, Kerala,

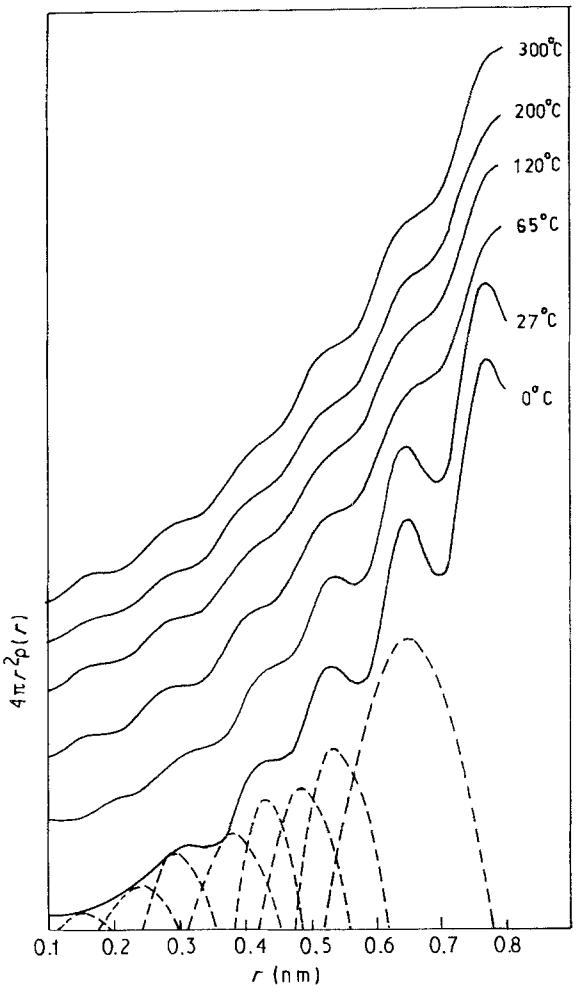

Figure 1 Radial distribution function of coir fibres for different temperatures of thermal treatment.

India. Fine uniform fibres of approximately 10–15 cm length were separated out, washed with distilled water and dried. The fibres were cut into small sizes of approximately 0.5 cm for treatments. The samples were divided for different treatments. For thermal treatment, small amount of sample were treated at temperatures of 0, 27, 65, 120, 200 and 300 °C, each for 2 h under a vacuum of 10^{-2} torr. For preparation of soda-cellulose, samples were treated with NaOH solutions of concentrations 5, 10, 15, 20 and 30% by weight for 2 h each. For mercerization, soda-cellulose samples were washed after treatment. They were then dried inside a desiccator for several days. A fine powder of the sample was made by grinding the finely cut sample in an agate mortar and pestle for a prolonged time and then passing it through a sieve of 200 mesh.

TABLE II Composition of coir fibre after it is subjected to different thermal, mercerization, and soda-cellulose treatments

Sample treatment	Particulars of treatment	Composition (wt %)		
		C	H	O
Heat treatment	0 °C	47.95	6.24	45.81
	27 °C	47.73	6.20	46.07
	65 °C	47.65	6.05	46.30
	120 °C	47.65	6.17	46.18
	200 °C	48.26	5.98	45.76
	300 °C	62.39	4.78	32.83
Mercerization	5%	45.71	6.05	48.95
	10%	46.55	6.39	47.06
	15%	46.28	6.24	47.48
	20%	46.42	6.20	47.38
	30%	46.10	6.20	47.70
Soda-cellulose	5%	38.99	5.45	55.56
	10%	37.34	5.27	57.39
	15%	38.88	5.46	55.66
	20%	38.02	5.45	56.53
	30%	39.77	5.63	54.60

Identification of the raw sample was carried out photographically by the X-ray powder diffraction technique using Cu K_α radiation with exposure for 24 h at 30 kV, 10 mA. Observed d values are listed in Table I. The sample is identified as mainly composed of cellulose I [7, 8].

Elemental analyses of the samples were carried out at CDRI, Lucknow and the results are given in Table II. The average electron density has been calculated on the basis of elemental analysis and the bulk density following the procedure described by Hofmann *et al.* [9]. This was necessary because we wanted to study the coir fibre as obtained for practical reasons as mentioned above.

X-ray diffraction profiles were recorded on a Philips diffractometer model PW 1729 using Ni-filtered Cu K_α radiation at 35 kV, 30 mA, for a 2θ scan at 0.5° min^{-1} and chart speed of 10 mm/2θ for 2θ = 5 to 90°. The background radiation was suppressed with the aid of a discriminator by running the diffrac-

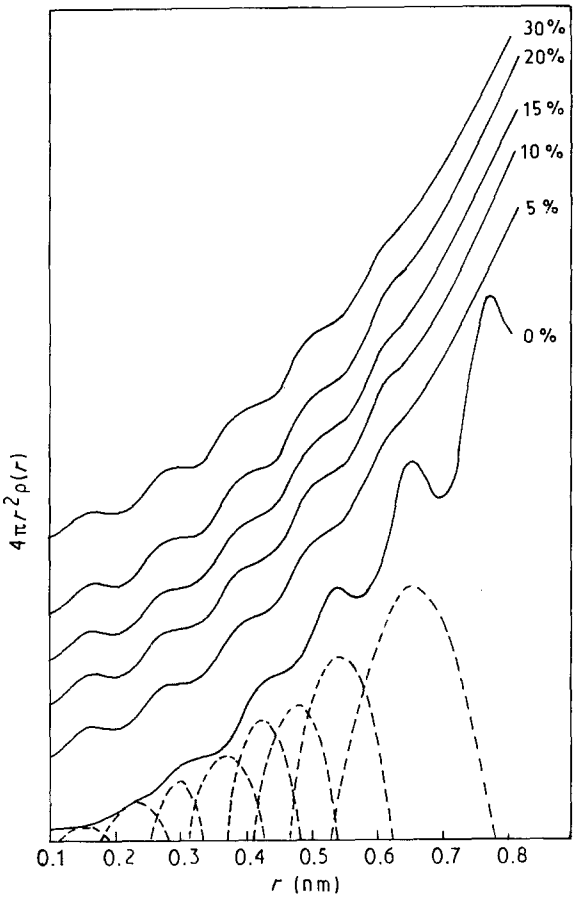

Figure 2 Radial distribution function of coir fibres for different concentrations of NaOH solution for soda-cellulose treatment.

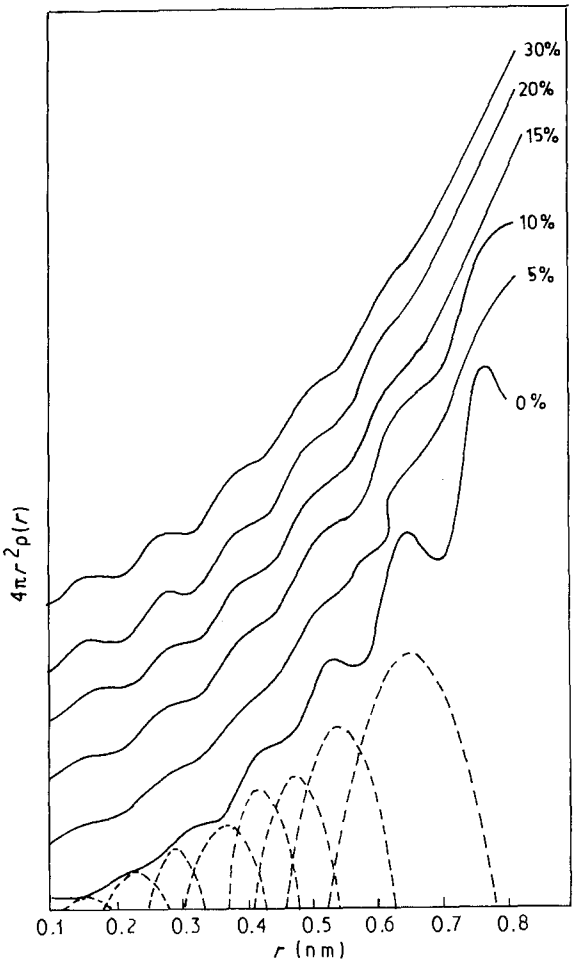

Figure 3 Radial distribution function of coir fibres for different concentrations of NaOH solution for mercerization treatment.

tometer once without a sample. Then the sample was mounted and the intensities recorded. Corrections for polarization and absorption were carried out using procedures described by Kaelble [10]. Tabulated values of atomic scattering factors [11] and incoherent scattering factors [12] were used for obtaining the independent scattering curves. The corrected intensities were scaled to electron units by the method described by Krough Moe [13]. The contribution of the flat-faced diffractometer sample in the small-angle region and that due to multiple scattering were subtracted by following the method described by Warren [14].

Following the procedure described by Kaelble [9], the radial distribution function (RDF) for polyatomic samples $4\pi r^2 \rho_e(r)$ is given by

$$4\pi r^2 \rho_e(r) = 4\pi r^2 \rho_{oe}(r) + \frac{2r}{\pi} \int_0^\infty S\, i(S)\, M_1(S)\, M_2(S)\, M_3(S) \sin(Sr) \cdot r\, dS$$

where

$$S = 4\pi \sin\theta/\lambda$$

$$i(S) = \frac{I_{obs}}{K} - \left(\sum x_i f_i^2(S) + \sum_i x_i I_{inc} \right)$$

where

$$k = \frac{\int S I_{obs}\, dS}{\int S(f^2 + I_{inc})\, dS}$$

and x_i = mole fraction of the atom of type i, $f_i(S)$ = atomic scattering factor of the atom of type i, I_{obs} = observed unscaled intensities, I_{inc} = incoherent intensity, $\rho_{oe}(r)$ = mean electron density of the bulk = $\rho_0[\sum x_i f_i(0)]$, $M_1(S)$ = sharpening factor = $\sum x_i f_i(0) / \sum x_i f_i(S)^2$, $M_2(S) = \exp(-bS^2)$ = artificial temperature factor introduced to suppress spurious peaks in RDF due to series termination errors, and $M_3(S) = 1$ for $S \leqslant S_{max}$ or 0 for $S > S_{max}$.

The RDF $4\pi r^2 \rho(r)$ gives the numbers of atoms between spherical shells of radius r and $r + dr$ with respect to an atom placed at the origin. For a perfectly disordered amorphous sample it is expected to rise monotonously. Because of the presence of local order

TABLE III Interatomic distances, coupling constants and r.m.s. displacements of the various bonds for various thermal treatments of the sample

Bonding	Temperature (°C)	Interatomic distance (nm)	Coupling constant	R.m.s. displacement
C1–C2, C5–O2, C6–O6	0	0.149	0.39	0.39
	27	0.149	0.36	0.43
	65	0.149	0.33	0.57
	120	0.150	0.32	0.35
	200	0.151	0.32	0.63
	300	0.151	0.35	0.77
C1–C3, C1–O2, C2–O5	0	0.240	0.50	0.84
	27	0.241	0.45	0.87
	65	0.241	0.40	0.89
	120	0.242	0.44	0.84
	200	0.242	0.38	0.94
	300	0.242	0.44	0.96
C1–C4, C2–C5, O1–O3′	0	0.290	0.37	0.24
	27	0.289	0.35	0.39
	65	0.290	0.38	0.84
	120	0.290	0.42	0.84
	200	0.291	0.37	0.87
	300	0.291	0.42	0.89
C1–C6, O2–O5, O1–O5′	0	0.368	0.56	1.05
	27	0.368	0.51	1.08
	65	0.368	0.45	1.10
	120	0.369	0.49	1.12
	200	0.370	0.43	1.14
	300	0.370	0.50	1.19
C2–C6, C2–C6′	0	0.428	0.46	0.71
	27	0.428	0.42	0.74
	65	0.429	0.37	0.77
	120	0.429	0.41	0.82
	200	0.430	0.36	0.84
	300	0.430	0.42	0.89
C1–O6, O1–O3, C1–O5′	0	0.478	0.57	1.08
	27	0.478	0.52	1.10
	65	0.478	0.45	1.12
	120	0.479	0.50	1.14
	200	0.479	0.44	1.16
	300	0.480	0.50	1.19

in structures, peaks are observed at positions corresponding to the interatomic distances.

Figs 1, 2 and 3 are the RDF profiles for different sets of studies undertaken. Fig. 1 shows the variation of RDF profile with temperature. Figs 2 and 3 show the variation with respect to the concentration of NaOH solution for soda-cellulose and mercerized fibres, respectively. When various interatomic distances in the sample are of the same order, then these peaks are not single but are composed of various overlapping peaks, each corresponding to a particular r value. Kaplow *et al.* [15] have shown that the distribution of atoms around their mean positions is Gaussian in nature. Therefore, the profile due to a particular r value should be of Gaussian type. Following their method, the RDF has been split into a set of Gaussian curves as shown by dotted lines in these figures for one case in each set.

Tables III, IV and V gives the positions of the peaks resolved for thermal, mercerized, and soda-cellulose treatments, respectively. These peaks have been identified by comparing with standard interatomic distance of various bonds as reported by Fink *et al.* [16].

As has been shown by Kaplow *et al.* [14] and Morimoto [17], the broadening of the peaks is a measure of the mean square deviation of the atoms from their mean position because of thermal vibration etc. The r.m.s. amplitude of vibration or mean square displacement can be obtained by the method described by them. The amplitude of vibration is inversely proportional to the strength of bonds and Kaplow *et al.* [15] have defined the coupling constant as $\gamma = (u^{-2}/u_\infty^{-2})^{1/2}$ where $(u_\infty^{-2})^{1/2}$ is the r.m.s. vibration of the atoms of very large separation. Thus $\gamma = 1$ for the completely uncoupled case and $\gamma = 0$ for the fully coupled case. Values of mean square displacement and coupling constants are also listed in Tables III, IV and V.

3. Results

The observed values of the interatomic distances do not exhibit any considerable change with a rise in the temperature of thermal treatment, as seen in Table III. Variation of coupling constant and r.m.s. displacement do not follow, in general, any regular pattern. However, in the case of first two interatomic distances, which play the most dominant role in bonding, there appears to be a downward trend in general up to

TABLE IV Interatomic distances, coupling constants and r.m.s. displacements of the various bonds for various concentrations of NaOH solution for mercerization of the sample

Bonding	Concentration of solution (%)	Interatomic distance (nm)	Coupling constant	R.m.s. displacement
C1–C2, C5–O2, C6–O6	0	0.149	0.36	0.43
	5	0.150	0.29	0.35
	10	0.150	0.30	0.30
	15	0.149	0.32	0.24
	20	0.149	0.31	0.17
	30	0.150	0.42	0.57
C1–C3, C1–O2, C2–O5	0	0.241	0.45	0.87
	5	0.242	0.33	0.63
	10	0.242	0.32	0.43
	15	0.241	0.35	0.47
	20	0.241	0.34	0.39
	30	0.242	0.45	0.66
C1–C4, C2–C5, O1–O3′	0	0.289	0.35	0.39
	5	0.290	0.35	0.71
	10	0.289	0.36	0.69
	15	0.289	0.39	0.66
	20	0.289	0.43	0.84
	30	0.290	0.71	0.87
C1–C6, O2–O5, O1–O5′	0	0.368	0.51	1.08
	5	0.367	0.40	0.96
	10	0.366	0.42	0.94
	15	0.366	0.42	0.92
	20	0.367	0.50	1.08
	30	0.367	0.60	1.19
C2–C6, C2–C6′	0	0.428	0.46	0.71
	5	0.428	0.37	0.84
	10	0.428	0.34	0.57
	15	0.427	0.36	0.54
	20	0.427	0.43	0.84
	30	0.428	0.42	0.96
C1–O6, O1–O3, C1–O5′	0	0.478	0.52	1.10
	5	0.477	0.43	1.08
	10	0.476	0.34	0.60
	15	0.476	0.33	0.35
	20	0.477	0.46	0.71
	30	0.477	0.42	0.84

around 120 °C, with a tendency to increase thereafter. For higher interatomic distances, where the order is likely to be less, the r.m.s. displacement values are increasing steadily with temperature, as expected, whereas the coupling constants vary without showing any regularity. Here also it is observed, in general, that the coupling constant attains a lower value at around 120 °C, as compared to other values. This behaviour is, possibly, due to expulsion of water molecules from the inter-chain space around this temperature which makes it a far more favourable conformation. It has been reported by Varma *et al.* [1, 2] that weight loss observed between 40 and 150 °C is due to evaporation of absorbed water. The conformation of the bonds in the ligno-cellulose complex at around 120 °C appears to be the most compact, which is likely to increase the mechanical strength of the fibre at this temperature. Above 200 °C coupling becomes weaker and consequently r.m.s. displacements are greater, as expected.

Mercerization has very little effect on interatomic distances as seen in Table IV. Ott *et al.* [18] and Clegg [19] have reported dimensional changes in cotton fibre on mercerization. That occurs, possibly, due to shrinkage of the interlayer distance due to mercerization. The possible reactions [18] between the alkali and the different constituents of coir fibre are that cellulose can absorb alkali from an aqueous solution and the absorbed alkali can be removed by soaking in water; the subsequent drying results in a change in physical properties without altering the chemistry of cellulose. Therefore, interatomic distances are not expected to show any significant change due to mercerization. Alkali can dissolve and leach out the fatty acids and their condensation products which form the waxy cuticle layer of the fibre. Excessive alkali treatment under more severe conditions can also damage the fibrils by removing the lignin hemicellulose which binds the cells in the fibre.

Alkali treatment at the first instant always tends to decrease the coupling constant and r.m.s. displacement. It is observed that coupling becomes strong and the r.m.s. displacement becomes less with rise in alkali concentration up to 10–15%, beyond which the reverse trend is followed for most interatomic distances. Strong coupling always results in increased mechanical strength. Prasad *et al.* [6] have reported that the mercerization process is affected by time and the concentration of alkali. The sequence of variations of

TABLE V Interatomic distances, coupling constants and r.m.s. displacements of the various bonds for various concentrations of NaOH solution for soda-cellulose treatments of the sample

Bonding	Concentration of solution (%)	Interatomic distance (nm)	Coupling constant	R.m.s. displacement
C1–C2, C5–O2, C6–O6	0	0.149	0.36	0.43
	5	0.150	0.36	0.57
	10	0.150	0.43	0.54
	15	0.149	0.31	0.43
	20	0.149	0.30	0.39
	30	0.150	0.36	0.60
C1–C3, C1–O2, C2–O5	0	0.241	0.45	0.87
	5	0.242	0.39	0.71
	10	0.242	0.42	0.47
	15	0.241	0.29	0.35
	20	0.241	0.38	0.84
	30	0.242	0.51	1.11
C1–C4, C2–C5, O1–O3′	0	0.289	0.35	0.39
	5	0.289	0.36	0.57
	10	0.289	0.43	0.54
	15	0.288	0.29	0.35
	20	0.288	0.35	0.66
	30	0.289	0.39	0.71
C1–C6, O2–O5, O1–O5′	0	0.368	0.51	1.08
	5	0.368	0.45	0.96
	10	0.368	0.54	0.92
	15	0.367	0.38	0.89
	20	0.367	0.41	0.94
	30	0.368	0.46	1.01
C2–C6, C2–C6′	0	0.428	0.46	0.71
	5	0.429	0.45	0.96
	10	0.429	0.54	0.92
	15	0.428	0.37	0.82
	20	0.428	0.46	0.99
	30	0.429	0.43	1.05
C1–O6, O1–O3, C1–O5′	0	0.478	0.52	1.10
	5	0.479	0.43	0.89
	10	0.479	0.48	0.71
	15	0.478	0.32	0.57
	20	0.478	0.41	0.96
	30	0.479	0.39	0.71

coupling constants, namely an initial decrease and then attainment of a saturation followed by an upward trend, in the present case seems to agree with the conclusion of Prasad *et al.* [6].

The soda-cellulose treatment (unwashed after treatment) produces an almost similar trend (Table V) with marginal variation in the corresponding values of mercerized samples (washed after treatment), which is, possibly, due to retention of alkali in the cellulose–lignin matrix.

4. Conclusions

On the basis of the results obtained in present investigation, we can conclude as follows:

1. The coupling constant is decreased on thermal treatment at around 120 °C. This results in better mechanical strength.

2. Mercerization with NaOH solution of concentration in the range 5 to 15 wt % is ideal for improving the strength of the coir fibre. At higher concentrations of NaOH solution the fibre becomes weaker and prone to rupture. These observations are in agreement with those of Prasad *et al.* [6].

References

1. D. S. VARMA, M. VARMA and I. K. VARMA, *Text. Res. J.* (December 1984) 327.
2. *Idem., Thermochim. Acta* **108** (1986) 199.
3. *Idem., J. Polym. Mater.* **3** (1986) 101.
4. *Idem., J. Reinf. Plast. Compos.* **4** (1985) 419.
5. K. G. SATYANARAYANA, C. K. S. PPILLAI, K. SUKAMARAN, S. G. K. PILLAI, P. K. ROHATGI and K. VIJAYAN, *J. Mater. Sci.* **17** (1982) 2453.
6. S. V. PRASAD, C. PAVITHRAN and P. K. ROHATGI, *ibid.* **18** (1983) 1443.
7. K. H. MEYER and L. MISCH, *Helv. Chim. Acta* **20** (1937) 232.
8. *Idem, Chem. Ber.* **70B** (1937) 266.
9. D. HOFMANN, P. WEIGEL, J. GANSTER and H. FINK, *Polymer* **32** (1991) 284.
10. E. F. KAELBLE, "Handbook of X-rays" (McGraw-Hill, New York, 1967) 22.1.
11. D. T. CROMER and J. T. WABER, *Acta Crystallogr. A* **18** (1965) 104.
12. F. HAJDU, *ibid.* **27** (1971) 73.
13. J. KROUGH MOE, *ibid.* **9** (1956) 951.
14. B. E. WARREN, "X-ray Diffraction" (Addison-Wesley, Reading Massachusetts, 1969) 116.
15. R. KAPLOW, T. A. ROWE and B. L. AVERBACH, *Phys. Rev.* **168** (1968) 1068.
16. H. FINK, B. PHILIPP, D. PAUL, R. SERIMAA and PAAKKARI, *Polymer* **28** (1987) 1265.
17. H. MORIMOTO, *J. Phys. Soc. (Jpn)* **13** (1958) 1015.
18. E. OTT, H. M. SPURLIN and M. W. GRAFFLIN (eds), "Cellulose and Cellulose Derivatives", Part II (Interscience, New York, 1954) p. 863.
19. G. G. CLEGG, *J. Text. Inst.* **15** (1924) 16.

Received 21 October 1991
and accepted 14 August 1992